Article

Application of SPR Method as an Approach to Gas Phase Sensing of Volatile Compound Profile in Mezcal Spirits Conferred by Agave Species

Araceli Sánchez-Álvarez [1], **Donato Luna-Moreno** [2,*] , **Oscar Silva-Hernández** [2] **and Melissa Marlene Rodríguez-Delgado** [3,4,*]

1   Departamento de Electromecánica Industrial, Universidad Tecnológica de León,
    Blvd. Universidad Tecnológica #225, Col. San Carlos, León 37670, Guanajuato, Mexico
2   Centro de Investigaciones en Óptica AC, Div. de Fotónica, Loma del Bosque 115, Col. Lomas del Campestre,
    León 37150, Guanajuato, Mexico
3   Facultad de Ciencias Químicas, Universidad Autónoma de Nuevo León,
    Av. Universidad S/N Ciudad Universitaria, San Nicolás de los Garza 66455, Nuevo León, Mexico
4   Centro de Investigación en Biotecnología y Nanotecnología (CIByN), Facultad de Ciencias Químicas,
    Universidad Autónoma de Nuevo León, Parque de Investigación e Innovación Tecnológica,
    Km. 10 autopista al Aeropuerto Internacional Mariano Escobedo, Apodaca 66629, Nuevo León, Mexico
*   Correspondence: dluna@cio.mx (D.L.-M.); melissa.rodriguezdl@uanl.edu.mx (M.M.R.-D.)

Abstract: Mezcal is a traditional Mexican spirit produced by distilling fermented agave, with a unique taste directly related to its volatile compound composition. Thus, the present research proposed the surface plasmon resonance (SPR) technique as a potential method to differentiate mezcals, studying several parameters at angular interrogations and at a fixed angle. The study evaluated eight mezcals from different agave species using SPR and gas chromatography-mass spectrometry (GC-MS). Despite the similarities in mezcal spirits corresponding to the same ethanol content and the same artisanal method, it was possible to obtain well-differentiated characteristics by SPR parameters, such as the width of the curve, the resonant angle, and reflectance intensities. Therefore, it was possible to demonstrate the potential use of the SPR technique as a rapid first approach to a screening test to differentiate types of spirits.

Keywords: surface plasmon resonance; mezcal; volatile compound profile; gas-phase; VOCs; SPR

1. Introduction

Mexico is characterized by its vast biodiversity of the *Agave* genus, which plays a crucial role in spirits production [1]. Alcoholic beverages from the *agavaceae* family are very popular in Mexico, and the fame of the tequila, produced from *agave tequilana* blue Weber, has transcended frontiers. However, mezcal is an artisan distilled alcoholic beverage that has continuously gained recognition and consumers worldwide. Mezcal spirits are produced in different regions of Mexico with a designation of origin, employing a variety of agaves, such as *A. salmiana*, *A. cupreata*, *A. duranguensis*, *A. fourcroydes*, *A. angustifolia*, and *A. potatorum* [2–4]. The artisan process of mezcal production involves the cooking of the agave stem (leafless axis), followed by the cooked stem's mashing, fermentation, and further distilling [4,5].

The quality and authenticity of mezcal, and any other distilled spirits, are the aroma compounds originating from the raw *agave* and the artisanal making process (fermentation, distillation, storage, and aging) [6,7]. Higher alcohols and esters produced by fermenting yeast cells are some of the aroma-active compounds responsible for fermented beverages' aroma [8–10]. These carbon-containing chemicals are part of a large group known as volatile organic compounds (VOCs), characterized by its low-molecular-weight (<300 Da), high vapor pressure ($\geq$0.01 kPa at 20 °C), and a high-to-medium hydrophobicity [11].

However, the absolute amount of VOCs is not relevant to the flavor of fermented alcoholic beverages, but the relationship (ratio) between the different volatiles, as synergy effects of the aroma-active substances, has been reported [12]. Currently, the gold standard for VOC detection involves the use of human sensory panels or gas chromatography coupled with mass spectrometry (GC-MS) [13–15]. Although using trained noses is very efficient for field studies, human panels yield biases and are prone to fatigue [15]. On the other hand, GC-MS is a highly accurate analytical method that separates, identifies, and quantifies different VOCs in a sample. However, it is well-known the high costs associated with the analysis, the difficulty of performing real-time on-site measurements, and the necessity of skilled operators [16]. Such a context has prompted an increased concern to work on developing affordable and reliable alternatives, such as artificial olfaction systems that overcome the drawbacks mentioned above.

Unlike mezcal, several studies on the composition of volatile compounds have been performed on tequila, reporting a broad number of volatile substances by gas chromatography [14,17,18], multivariate analysis of FTIR spectroscopy [19], Raman spectroscopy [20], and UV–vis absorption spectroscopy [21]. Each of these techniques provides different information about the constituents or other characteristics of the alcoholic beverages, complementing its characterization and further authentication. In this sense, the detection of VOCs in the gas phase has already been demonstrated by the SPR technique [22–25]. Especially when using air as the analysis medium, its low optical index diminishes the noise during the detection, allowing a high signal/noise ratio [15]. The surface plasmons formed on a metallic surface have an absorption peak at a specific wavelength. By adsorbing VOCs to the surface, the position of the resonance notch is shifted. When this happens, the resonance notch's width and depth can also be changed [26]. These parameters characterize the resonance perturbation and can be associated with the dielectric medium's optical properties [26]. Thus, the present research proposes the surface plasmon resonance (SPR) technique as a qualitative method to differentiate mezcals, studying in the vicinity of the absorption band of the different VOC profiles in the gas phase of the spirits. The reflectivity, as a function of two parameters, width and resonant angle, was measured by analyzing the resonant angle of the SPR curve produced by the attenuated total reflection in the Kretschmann configuration.

Studies by Vera-Guzmán et al. [4] established that volatile compounds in mezcal differed between *Agave* species, place of origin, production season, and fermentation conditions, showing that composition varied significantly among artisanal distilleries. Therefore, samples were collected from bottled spirits from a well-known trademark, Gracias a Dios^{MR} (Thankgod) [27], assuring the agaves were from the same region in Matatlán (Oaxaca, México) under identical production conditions in the artisanal distillery. In the study, eight different mezcals were tested, produced from six agave plants from Mexico: *Agave Americana* var. *oaxacensis* (AA), *Agave karwinskii* (AK), *Agave potatorum* (AP), *Agave angustifolia* Haw, *Agave marmorata*, and *Agave rhodacantha*. The volatile compounds of the samples were characterized using gas chromatography (GC-MS) and the proposed SPR method.

2. Materials and Methods

2.1. Mezcal Samples

The samples were obtained from the artisanal distillery Gracias a Dios (Thankgod), from the region of Matatlán, Oaxaca (longitude: O96°22′57.4″, north latitude 16°51′52.92″, and an altitude ranging from 1500 to 2900 m above sea level). The samples were taken from bottles of 750 mL of white mezcal (without aging) with an alcohol content of 45%. The eight samples were produced from different agave plants: madre cuishe (*A. karwinskii*), coyote (*A. americana*), tepeztate (*A. marmorata*), tobalá (*A. potatorum*), arroqueño (*A. americana*), mexicano (*A. rhodacantha*), cuishe (*A. karwinskii*), and espadín (*A. angustifolia Haw*). The agave varieties employed in the mezcal production range were aged 25 (*A. marmorata*),

15 (*A. americana*), 13 (*A. karwinskii and A. potatorum*), 10 (*A. rhodacantha*), and 8 (*A. angustifolia Haw*) years. All samples were kept at 8° until their analysis.

2.2. Extraction of Volatile Compounds

Volatile compounds were extracted by liquid–liquid extraction, using 15 milliliters of mezcal with 15 mL of dichloromethane of ≥99.9% purity (Sigma, St. Louis, MO, USA). Subsequently, the samples were mixed and centrifuged for 10 min at 5000 rpm. Finally, the organic extract was separated and dried using anhydrous sodium sulfate of ≥99.0% purity (Sigma, St. Louis, MO, USA) and then concentrated to a volume of 1.5 mL with a rotatory evaporator (IKA, Wilmington, NC, USA).

2.3. Analysis of Volatile Compounds Using GC-MS

The extracts were analyzed by Gas Chromatography-Mass Spectrometry (GC-MS) in a 6890N Network system (Agilent Technology, Santa Clara, CA, USA), coupled to a quadrupole selective mass spectrometer detector 5975 (Agilent Technology, USA) with an electronic impact ionization system at 70 eV and 260 °C. An HP-FFAP column of 25 m × 0.32 mm (i.d), 0.52 μm film (Agilent Technologies, Santa Clara, CA, USA) was employed for compound separation. High-purity helium was used as a carrier gas at 1 mL/min flow. The GC oven temperature was programmed as follows: 40 °C for 5 min, which was increased by 20 °C/min to 100 °C and maintained for 1 min. The temperature was then increased to 230 °C by a second rate of 3 °C/min and kept for 40 min. The injector was operated in splitless mode at 230 °C. The compounds were identified by comparing their mass spectra with the National Institute of Standards and Technology (NIST98) database with a match of at least 80%. Each compound's average relative abundance (n = 3) was reported as a percentage of the normalized area of the corresponding peak.

2.4. SPR Measurements with Angular Interrogation

In the first experiment, the response of the sensor upon VOC injection was monitored by measuring the shift in the resonance angle. The SPR measurements were performed using a homemade optical platform based on a Kretschmann configuration and a *p*-polarized laser light (N-LHP, Newport Corp., Irvine, CA, USA) at a wavelength of 633 nm to excite the surface plasmons. A hemicylindrical-shaped prism, made of FK5 glass, was coated on its flat surface with a thin silver film of 50 nm, estimated using a quartz crystal thickness monitor (XTC/2 Depositions Controllers Leybold Inficon quartz monitor, San Jose, CA, USA). The thermal evaporation was performed in a vacuum chamber (High Vacuum Coating Plant BA510, Balzers High Vacuum Corp., Santa Ana, CA, USA) using silver pellets (purity of 99.99%, Kurt J. Lesker Co., Clairton, PA, USA). Silver was evaporated at a rate of 5 Å/s in an atmosphere of 8×10^{-6} mbar [28]. The prism was mounted with its flat face on the base of the superior plate of two stacked rotation plates, driven by a stepper motor (FCR100, Newport Corp., Irvine, CA, USA). The coupled signal, obtained from the light launched into the prism, was reflected at the metal film to a silicon photodetector (Hamamatsu, Bridgewater, NJ, USA) mounted on a lower-stage rotator. Meanwhile, the prism's silver coating was facing the flow Teflon cell, which had an inlet and outlet that allowed the sample to encounter the sensing surface through its inner channel (see Figure 1a). The solutions were pumped by a syringe pump (Legato 100, KDScientific, Boston, MA, USA) at a rate of 100 μL min^{-1}. The photodetector provided a voltage signal proportional to the intensity of the incident light, which later was converted into a digital signal in the interface unit (USB 6003, National Instruments, Ciudad Juárez, México). Angular scans were performed for every sample to register the resonant angle corresponding to the reflected light's minimal intensity. This angular interrogation was performed for every mezcal solution by measuring the shift in the resonance angle, enabling the characterization of small refractive index changes.
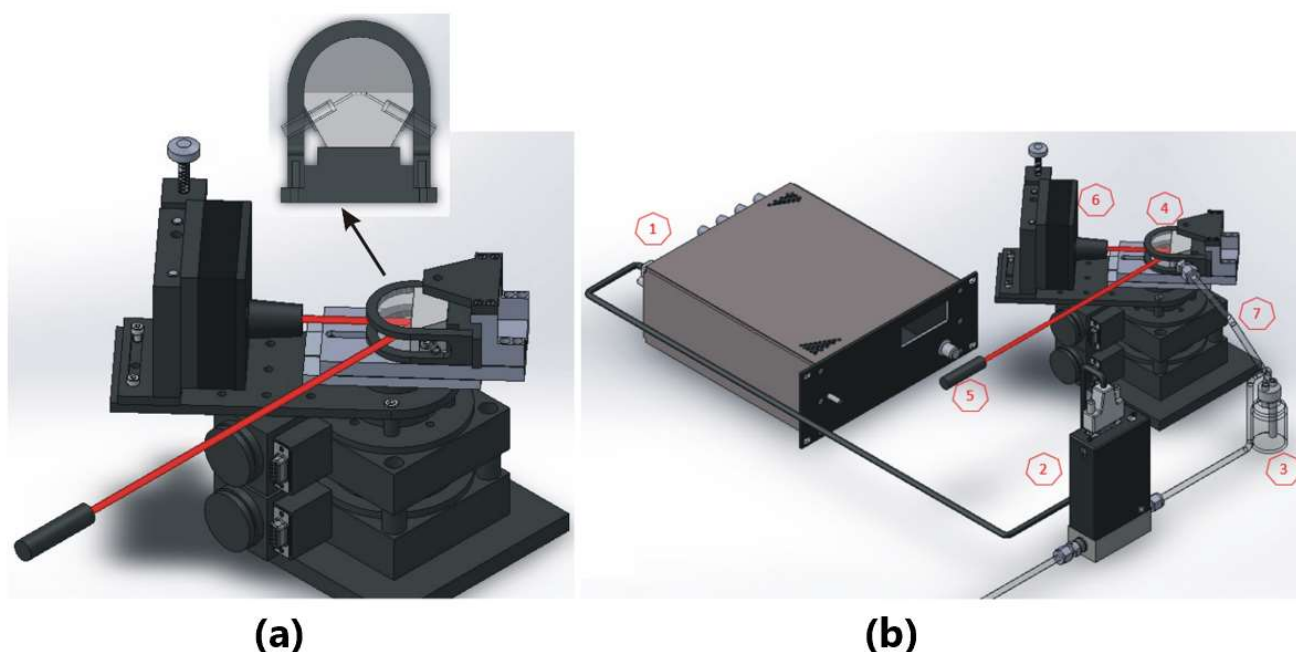
Figure 1. (**a**) Experimental setup of the SPR sensor for angular interrogation (liquid samples) and (**b**) SPR scheme for intensity interrogation approach (gaseous samples). The system is integrated by a (1) mass flow controller, (2) metal-sealed pressure flow controller, (3) sample container, (4) silver-coated prism coupled to flow cell, (5) He-Ne laser, (6) photodetector, and (7) stepper rotating stage.

2.5. SPR Measurements at a Fixed Angle

The custom-built gas phase SPR platform is shown in Figure 1b, working under an intensity interrogation approach. The refractive index variations of the gas phase were detected as a change in the reflectance units at a fixed incident angle. This working angle was established at the highest slope of the linear region of the plasmon curve (approaching the critical angle of the minimal intensity of reflected light), which is the region of interest due to its sensitivity to changes in light intensity. The reflectance intensity was monitored as a function of time during the measurement of the mezcal samples. A fluidic system was employed for controlled injection of gas phase analyses, implemented with a mass flow and pressure controller (MKS Instruments, Inc. Andover, MA, USA). The airflow was set at 0.001 sccm and bubbled in one milliliter of the sample (contained in bottles of 10 mL). The flow conditions were maintained to ensure the air carrier flow through the head space to allow the sample to encounter the SPR detection system. Once a measurement concluded, a purge step was performed between mezcal samples, flowing air over the sensor surface for 5 min to dissipate the residues that may have remained in the flow cell. The gas phase of methanol and ethanol solutions was also measured as a reference.

2.6. SPR Theoretical Simulations by Fresnel Equations and the Matrix Method

The optical properties of thin films are commonly calculated by the Fresnel equations and the matrix method, where the electric and magnetic fields are expressed as column vectors and each film as a transfer matrix. Then, the obtained amplitudes at the emergent interface are associated with the transmitted wave (no returning wave in the emergent medium) [29]. The SPR can be expressed as Equation (1):

$$\begin{bmatrix} B \\ C \end{bmatrix} = \begin{bmatrix} cos\delta & \frac{isin\delta}{\eta} \\ i\eta sin\delta & cos\delta \end{bmatrix} \begin{bmatrix} 1 \\ \eta_s \end{bmatrix} \tag{1}$$

where B and C correspond to the amplitude of the normalized electric and magnetic fields, respectively, and δ is the phase thickness (given as $\delta = 2\pi n d(\cos\theta)/\lambda$, where d is the

physical thickness, η is the refractive index of the silver thin film, λ is the wavelength, η_S is the refractive index of the substrate or sample medium, and θ is the angle for the incident medium). Y is the admittance of the assembly system ($Y = C/B$). The reflectance amplitude r is given for Equation (2).

$$r = \frac{\eta_0 - Y}{\eta_0 + Y} \tag{2}$$

Meanwhile, the theoretical reflectance is expressed as Equation (3).

$$R = |r|^2 = \left| \frac{\eta_0 - Y}{\eta_0 + Y} \right|^2 \tag{3}$$

where η_0 is the refractive index of the exit medium (corresponding to air). Finally, the solution is reduced to finding the reflectance of the simple ideal interface between an incident medium η_0 and a medium of admittance Y. The refractive index calculation is found by fitting the theoretical and experimental SPR curves using the method of least squares [30].

3. Experimental Results

3.1. Analysis of Volatile Compounds Using GC-MS

All the mezcal brands analyzed correspond to white mezcal type, bottled just after distillation (no aging process), and leveled at 45% v/v, established as a control quality standard by the producer. Furthermore, all mezcal samples were obtained from the same artisanal factory (Gracias a Dios, Thankgod) and produced under the same fermentation method. The volatile organic compounds were obtained by liquid–liquid extraction and identified by GC-MS in eight mezcal samples obtained from six agave species. Table 1 summarizes the volatile compounds profiles of mezcals types, showing as primary compounds alcohols, esters, and organic acids.

High alcohols (above 2C), such as 1-propanol, isobutyl alcohol, and isopentyl alcohol, were common in all samples. These compounds have been reported to be responsible for the sweet notes in alcoholic beverages and are produced by microorganisms' catabolism of amino acids [31]. Notably, 1-propanol was the most predominant alcohol in all samples, showing a high variability among them. On the other hand, the alcohol 2-butanol was not detected in two samples, "Madre Cuishe" and "Coyote", produced from *A. karwinskii* and *A. americana* agave plants, respectively. The presence of 2-butanol might be related to the young age of the agaves as "Coyote" was produced from a seven-years-old agave. Meanwhile, "Madre Cuishe" was obtained from a 13-years-old agave. In this sense, the highest amount of 2-butanol was presented by the mezcals produced from the oldest agaves, *A. marmorata* at 25 years old (mezcal "Tepeztate") and *A. americana* at 15 years old (mezcal "Arroqueño").

Meanwhile, a group of carboxylic acids, varying from acetic acid (C2) to valeric acid (C5), were found in all analyzed samples. The diversity in the presence of these compounds is pretty standard and has been reported in different alcoholic beverages, such as beer [32] and tequila [33].

Table 1. Relative abundances of volatile compounds in mezcal by different *Agave* origins of the eight mezcals analyzed.

Agave Specie / Agave Ripeness (Years)	A. Karwinskii		A. marmorata	A. potatorum	A. rhodacantha	A. angustifolia	A. americana	
	(13)	(13)	(25)	(13)	(10)	(8)	(7)	(15)
Mezcal Sample / Compounds	Madre Cuishe	Cuishe	Tepeztate	Tobalá	Mexicano	Espadín	Coyote	Arroqueño
1-Propanol	47.85	7.98	32.86	25.95	62.03	5.88	31.82	35.5
Isobutyl alcohol	2.32	16.97	4.06	7.26	2.61	8.33	8.59	4.92
Cyclopentanone	0.35	0.05	0.47	0.47	0.17	0.41	0.52	0.15
Isopentyl alcohol	11.9	42.33	21.17	39.93	16.35	54.71	39.89	20.17
β-Ethoxypropionaldehyde diethyl acetal	0.1	0.25	0.38	0.44	0.3	0.14	0.26	0.65
Cyclopentanol	0.18		0.19	0.16	0.12		0.29	
Cyclopentanol, 2 methyl trans	0.12		0.16	0.18	0.12	0.11	0.23	0.1
Ethyl (S)-lactate	4.04	4.23	3.47	1.98	2.51	1.98	4.95	2.21
Acetic Acid	9.84	19.66	18.22	8.56	14.29	22.06	8.6	7
Furfural	0.39	1.25	0.32	0.2	0.28	0.28	0.3	0.18
Propanoic acid	0.93	0.27	1.38	0.58	0.65	0.22	0.24	0.48
Isobutyric acid	0.3	0.55	0.22	0.06	0.16	0.14	0.1	0.26
2-Furaldehyde, 5-methyl	0.52	0.9	0.42	0.24	0.36	1.13	0.71	0.13
Isovaleric acid	0.54	0.26	0.44	0.41	0.33	0.45	0.41	
α-Terpieol	0.51	0.28	0.42	0.06	0.32		0.19	1.08
Valeric acid, 3 methyl							0.24	
Furfuryl alcohol		0.15	0.17	0.19		0.05	0.18	
2-Butanol		1.12	20.08	9.33	15.69	0.81		16.65
Butanoic acid, ethyl ester			0.09	0.11				
Butanoic acid		0.2	1.76	1.73		0.4		
α-methyl-α-[4-methyl-3-pentenyl] oxiranemethanol								0.15
Terpineol								0.2
Decanoic acid, ethyl ester								0.23

However, it highlights the variability in the orders of magnitude of the amount of acetic acid, clearly observed in all the samples, compared with the homogeneity of concentration of other carboxylic acids. Interestingly, in all types of mezcal, a high concentration of propanol corresponded to a low acetic acid amount present in the sample. This behavior was previously reported in the work of Vera-Guzmán et al., where the effect of ammonium sulfate was evaluated in the kinetic profile of volatile compounds of mezcal obtained by artisanal fermentation [4,5]. The study showed that the fermentative microorganisms' response to nitrogen availability resulted in increased propanol production and reduced concentration of acetic acid [5]. A similar tendency was observed in the tequila fermentation process by *A. tequilana* musts [33–35], attributed to a higher reduced sugar consumption induced by nitrogen. The nitrogen acted as a sugar transporter and protein synthesis inductor during fermentation, thus promoting the growth of microorganisms in the media [33]. From the results obtained in this study, a propanol/acetic acid ratio was calculated and is summarized in Table 2, showing that "Arroqueño", "Madre Cuishe", and "Tobala" mezcal presented the highest ratio.

Table 2. Ratio of the relative abundances of 1-propanol and acetic acid in mezcal samples.

Mezcal Sample	1-Propanol (%)	Acetic Acid (%)	Propanol/Acetic Acid Ratio
Madre Cuishe	62.03	14.29	4.34
Tobala	47.85	9.84	4.86
Arroqueño	35.50	7	5.07
Tepeztate	32.86	18.22	1.80
Coyote	31.82	8.6	3.70
Mexicano	25.95	8.56	3.03
Cuishe	7.98	19.66	0.41
Espadín	5.88	22.06	0.27

On the other hand, mezcal produced from *A. potatorum*, *A. marmorata*, and *A. rhodacantha* showed the highest amounts of higher alcohols (1- propanol, isopentyl alcohol, cyclopentanol, and 2-butanol). Meanwhile, terpineol, α-methyl-α-[4-methyl-3-pentenyl] oxiranemethanol, and decanoic acid ethyl ester were unique compounds found in samples of "Arroqueño" mezcal, produced from agave *A. americana* of 15-years-old. The same occurs with valeric acid ethyl ester, detected only in "Coyote" mezcal, also made from *A. americana*, but at seven-years-old. In those cases, these changes in concentration and the presence of unique compounds could be used as an alternative for the classification of mezcal types, acting as authentic markers of origin, potentially attributed to the agave specie but also its ripeness. For example, the presence of chain acid ethyl esters, such as decanoic acid ethyl ester, has been reported that may stem from the agave plant, varying in each species and synergizing to produce the unique mezcal aroma [36]. However, more analysis of mezcal samples is necessary to establish a good concentration pattern for a specific classification.

3.2. SPR Measurements with Angular Interrogation

Usually, a BK7 glass prism (n = 1.51509 for λ = 632.8 nm) is employed in conventional SPR systems; however, all mezcal samples are transparent (white mezcal) and contain the same amount of ethanol (45% *v/v*). Thus, the solution presents a refractive index predominantly real, expecting similar optical characteristics. Therefore, to increase the sensitivity of the SPR system, an FK5 glass prism with a lower refractive index was employed (n = 1.48601, λ = 632.8 nm). The FK5 prism allows the differentiation of the optical responses by changing the sensitivity of the SPR system from 170 to 180°/RIU (refractive index units) [37].

The system was calibrated with air (n = 1), distilled water (n = 1.3324 [38]), methanol (n = 1.3292 [38]), and ethanol (n = 1.35803 [38]). SPR measurements were performed at room temperature at 25 °C. These references characterized the thin silver film deposited on the FK5 prism, obtaining a value of d = 504 Å and N = $n - ik$ = 0.06656 − 4.0452i, which

corresponds to that established in the literature [39]. Furthermore, the method of least squares was applied to the theoretical and experimental SPR curves obtained, allowing the determination of the refractive index of the samples. Figure 2 shows the SPR curves of the mezcal samples and the reference solutions (water, methanol, and ethanol). As can be noticed from the SPR curves of the mezcal samples, resonant angles are in the region of 74–74.7°, between the angles corresponding to water or methanol (which have very similar refractive indices) and ethanol reference solutions. It is worth noting that a minimum dip displacement, between methanol and water, was expected, due to the close proximity on their refractive indices [38]. In our study, we obtained a calculated refractive index (see Table 3) of $n = 1.3284$ for methanol (an error of 0.06% compared to the reference) and $n = 1.3293$ for distilled water (an error of 0.23% compared to the reference). Regarding the difference between the lowest points in their SPR curves, the water presents a higher reflectance minimum (R_{min}) attributed to the absorbing effect of this medium, in comparison with methanol, a non-absorbing dielectric [40]. This effect occurs when the absorption peak of the outer medium coincides with the plasmon resonance wavelength [40].
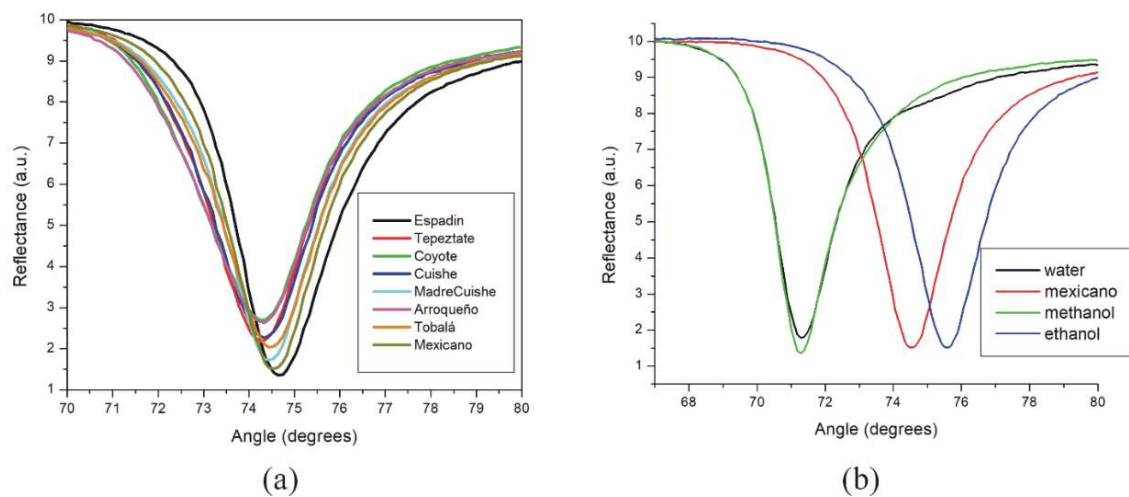

(a)   (b)

Figure 2. SPR curves at sweep angle of (**a**) eight mezcal samples and (**b**) water, methanol, and ethanol solutions measurements with "mexicano" mezcal sample as reference for pointing to the resonant angles region of the samples.

Table 3. SPR curve parameters of mezcal samples and reference solutions.

Mezcal Samples	Resonant Angle (Degrees)	Width (Degrees)	R_{min}	Refractive Index (n)
Arroqueño (*A. americana*)	74.441	3.052	2.650	1.3472
Coyote (*A. americana*)	74.357	3.082	2.70	1.3468
Cuishe (*A. karwinski*)	74.333	2.758	2.285	1.3474
Madre Cuishe (*A. karwinski*)	74.551	2.303	1.576	1.3484
Espadín (*A. angustifolia* Haw)	74.723	2.699	1.345	1.3504
Mexicano (*A. rhodacantha*)	74.627	2.567	1.506	1.3493
Tepeztate (*A. marmorata*)	74.339	2.771	2.195	1.3469
Tobalá (*A. potatorum*)	74.543	2.681	2.039	1.3482
Methanol	71.374	2.213	1.373	1.3284
Distilled water	71.454	2.195	1.768	1.3293
Ethanol	75.598	2.686	1.511	1.3556

Several parameters were extracted from the experimental SPR curves, such as the curve's width, minimum intensity (R_{min}), and resonant angle. These parameters characterize the resonance perturbation attributed to the optical properties of the dielectric medium, allowing the calculus of the refractive indices of each mezcal sample by Fresnel equations. The SPR curve parameters are summarized in Table 3.

From the calculated *n* values, the highest refractive index was presented by "Espadin" mezcal, *n* = 1.3504 (θsp = 74.7231 degrees), which was expected as it possesses the highest proportion of isopentyl alcohol (higher alcohol of 5 carbons). In addition, "Madre Cuishe" and "Tobala" mezcal presented a high refractive index, highlighting their 1-propanol (alcohol of 3 carbons) content as 62% and 47.8%, respectively. According to the literature, the increase in alcohol refractive index occurs as the number of carbon atoms (N) of the alcohol increments [41]. Furthermore, the resonant angle of the SPR curve is directly related to the refractive index; thus, the augment in this parameter is reflected as a shifting of the resonance notch toward higher angles. For the rest of the mezcals, the refractive index values were very similar (ranging from 1.3468 to 1.3472), making it difficult to establish a direct correlation with the volatile compounds profile obtained from the GC-MS analysis. It is noteworthy the possibility that other compounds were present, and they were not identified by GC-MS analysis performed in this work, as the sample of mezcal "Mexicano" showed a high refractive index and resonance angle displacement. However, there is no apparent match with its volatile compound profile. Thus, more analysis of this mezcal sample would be necessary to establish a valid SPR characterization.

Meanwhile, in terms of the SPR curve's width and depth (R_{min}), these parameters are influenced by the imaginary part of the refractive index (extinction coefficient) [42]. Typically, at the resonance angle, the reflectance tends to decrease to almost zero due to the evanescent wave decaying provoked by the total internal reflection condition in the system [40]. When the sample is a non-absorbent medium, the SPR curve tends to be narrow and deep (lowest R_{min}). Meanwhile, broad SPR curves with increasing reflectance minimum intensities (high R_{min}) indicate the presence of strongly absorbing species in the sample [43]. This effect occurs when the absorption peak of these species coincides with the plasmon resonance wavelength, weakening the evanescent field that causes a plasmon inhibition and, thus, an SPR curve less pronounced [40].

In this sense, it can be observed that despite all samples corresponding to white mezcal (transparent solutions without aging process), significant differences in R_{min} values are presented. For example, "Arroqueño" and "Coyote" samples showed the highest values of width and depth (R_{min}), indicating that they possess more absorbing components that make them absorbent mediums. Interestingly, "Coyote" and "Arroqueño" spirits were obtained from the same agave specie (*A. americana*), which might indicate that the agave species could confer the absorbent compound profile in these mezcals.

Then, as it is observed, the SPR curve pattern is not exclusively determined by the alcohol contents in the sample but derived from the interaction of the components in the volatile compound profiles. Therefore, an additional multiparameter analysis was performed in all the samples, plotting the SPR parameters obtained to establish their common properties. The results are observed in Figure 3, showing how some samples are naturally grouped accordingly to their similarities. From the multiparameter analysis, it is clearly observed that "Coyote" and "Arroqueño" spirits present similar refractive index (resonant angle) and are the most absorbent mezcals (higher width and depth), and, despite the rest of the mezcals possessing refractive index values very close to each other, a group integrated by "Cuishe", "Tobala", and "Tepeztate" can be observed, intermediate in levels of transparency. Finally, "Madre Cuishe", "Espadin", and "Mexicano" correspond to the group of mezcals that are more transparent (fewer absorbent components).
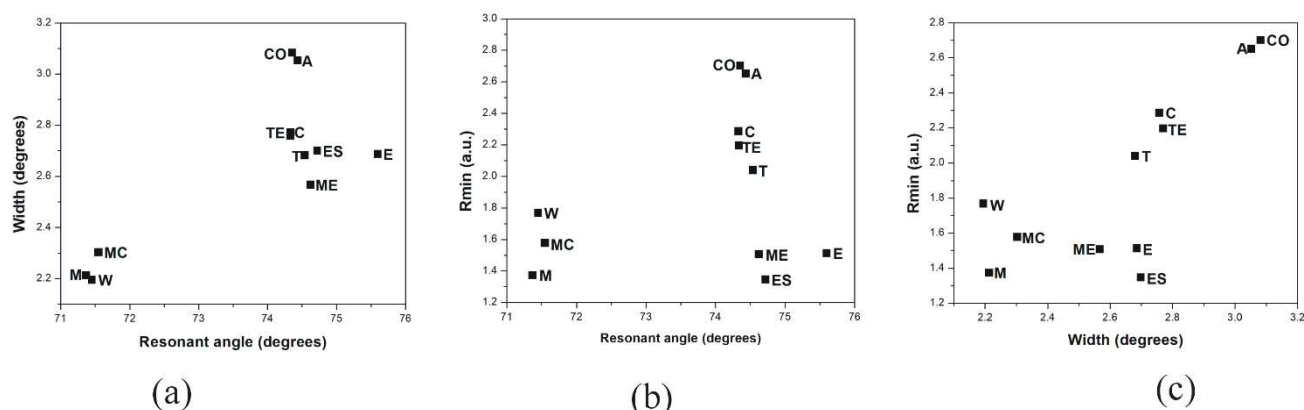
(a)   (b)   (c)

Figure 3. Multiparameter analysis of SPR parameters extracted from mezcal curves. (**a**) Plot of width vs. resonant angle, (**b**) R_{min} vs. resonant angle, and (**c**) R_{min} vs. width. The samples nomenclature corresponds to the mezcal samples: espadín (ES), tobalá (T), cuishe (C), tepeztate (TE), mexicano (ME), arroqueño (A), madre chuishe (MC), and coyote (CO), and the reference solutions: distilled water (W), methanol (M), and ethanol (E).

Finally, from the SPR curve parameters, a sensitivity and detection accuracy analysis of the proposed sensor was also performed. The accuracy of the detection is mathematically established in Equation (4) as the reciprocal of the width of the SPR curve ($\delta\theta$ 0.5) at half maximum reflectance, represented as

$$DA = \frac{1}{\delta\theta 0.5} \tag{4}$$

In this sense, high accuracy is obtained from the narrow width of the SPR curves [44]. On the other hand, the sensor sensitivity is related to the instrumentation and is calculated according to Equation (5) [45]

$$S\Delta_\theta = \frac{\Delta\theta_{res}}{\Delta n} \tag{5}$$

where $\Delta\theta_{res}$ and Δn correspond to the variation in resonance angle and refractive index, respectively. The overall performance parameters are tabulated in Table 4, showing notable results compared to other sensors established in the literature. Interestingly, the proposed sensor exhibits one of the highest sensitivities, only below Al- and Au-graphene-based sensors. In terms of detection accuracy, it shows an average performance compared to bare gold and the Au-graphene sensor. The highest accuracy was reported by Maharana et al. using thin films of gold (Au), silver (Ag), and aluminum (Al) on silicon prisms [46]. For the best sensing performance, the sensitivity and detection accuracy is expected to be as high as achievable [47].

Table 4. Comparison of sensing performance of SPR sensors.

Type of SPR Sensor	Sensitivity (Degrees/RIU)	Detection Accuracy (Degrees^{-1})	Reference
Gallium phosphide prism + gold (50 nm) + silicon (9 nm)	37.08	0.225	[48]
N-FK51A prism + gold (55 nm) + graphene (0.34 nm)	275.15	1.41	[44]
Silicon prism + gold (50 nm)	58	1.8	
Silicon prism + silver (50 nm)	138	4.9	[46]
Silicon prism + aluminum (50 nm)	377	23.3	
Fiber optic + gold (40 nm) + graphene (0.34)	33.98	0.298	[49]
FK5 Prism + silver (50 nm)	164.27	0.37	Present work

3.3. SPR Measurements at a Fixed Angle

The mezcal samples were also characterized under the intensity interrogation approach in a custom-built gas-phase SPR platform, allowing the measurement of the refractive index variations (intensity of reflectance) of the gas phase of the sample. The working angle was established at the highest slope of the linear region of the plasmon curve; the measurements were monitored as a function of time. Figure 4 shows the SPR intensity responses of the samples and reference solutions (methanol, ethanol, and air). Interestingly, the mezcal samples showed a tendency effect between the propanol/acetic acid ratio (shown in Table 2) and the reflectance intensity presented by the SPR measurement. Therefore, a standard Pearson correlation test was performed to establish the significance level in the results, obtaining a coefficient of 0.82847, which indicates a high correlation.
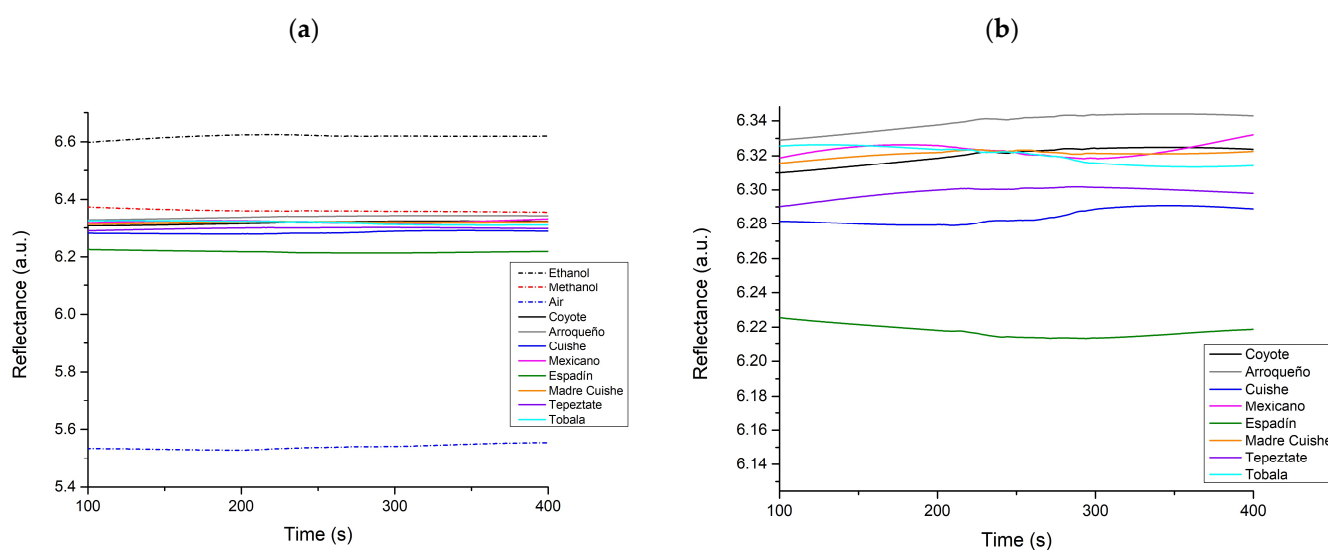
(**a**)　　　　　　　　　　　　　　　　　　　　　　　　(**b**)

Figure 4. SPR measurements at a fixed angle: (**a**) mezcal samples and reference solutions (methanol, ethanol, and air) and (**b**) zoom of the SPR response region of mezcals.

It is observed that a high concentration of propanol corresponded to a low acetic acid amount present in the sample. This behavior was previously reported in Vera-Guzmán et al., where the effect of ammonium sulfate was evaluated in the kinetic profile of volatile compounds of mezcal [5].

Unfortunately, as can also be seen in Figure 4, fluctuations are displayed in the SPR signal recordings over time. This effect is attributed to instability in the injection system that supplies the platform's flow, causing turbulent flows instead of laminar. In this sense, Table 5 shows some advantages and disadvantages of plasmonic-based sensors compared to other potential technologies in this field.

Table 5. Comparison of latest sensing technologies used in aquaculture.

Sensing Technology	Advantages	Disadvantages	References
Gas chromatography coupled with mass spectrometry	High sensitivity High accuracy High repeatability	Technical expertise required Costly reagents. Time-consuming. Impossibility of in-field detection	[50]
Prism-based SPR	Allows label-free detection Highly sensitive to the refractive index of the medium Widely established and commercially available Allows multiplex analysis	Difficulties for miniaturization Only detects refractive index changes close to the metal film surface High requirements for temperature control Difficulties for remote sensing applications.	[51]

Table 5. *Cont.*

Sensing Technology	Advantages	Disadvantages	References
Fiber Optic-SPR	Label-free detection Ease of miniaturization. Flexible and easy moving Allows remote sensing Low requirements for temperature control Allows multiplex analysis	Complex fabrication and surface functionalization Damage of molecules due to prolonged exposure to incident light Slow response time due to the diffusion effect of analytes.	[52,53]
Localized-SPR	Allows multiplex analysis and miniaturization Allows the improvement of the optical properties of the systems by varying the nanoparticles' size, shape, and composition. Allows the use of wavelengths that do not overlap with the spectral features of strongly absorbing mediums	Only detects refractive index changes at tens of nanometers into the surrounding medium. Detection at the single-molecule level	[45]
Electrochemical sensors	Low-cost production of electrodes and microelectronic circuits. Straightforward interface of electronic read-out and processing	Electrical interference effects High effect on sensor's response due to pH and ionic strength in the sample Increase in the signal-to-noise due to miniaturization Requirement of redox molecules to mediate the electrochemical reactions Fouling effects on the electrodes	[54]

4. Conclusions

This work evaluated the potential use of the SPR technique as a simple and rapid test for the optical characterization of different mezcal samples. Despite the similarities in mezcal spirits corresponding to the same ethanol content and the same artisanal method, it was possible to obtain well-differentiated characteristics by SPR parameters, such as the width of the curve, the resonant angle, reflectance intensities, or refractive indices. These optical characteristics could help to create patterns or fingerprints associated with mezcal properties, obtaining a collective amount of information to capture an entire complex aroma or even as a mark indicative of authenticity. Thus, the proposed method is explored to complement the existing standard chromatographic techniques, providing a rapid first approach to a screening test to differentiate types of mezcals. However, more analysis of mezcal samples will be necessary to establish a good pattern for a specific classification.

Author Contributions: Conceptualization, A.S.-Á. and D.L.-M.; Methodology, A.S.-Á., O.S.-H. and D.L.-M.; Formal Analysis, D.L.-M. and M.M.R.-D.; Investigation, A.S.-Á., O.S.-H., D.L.-M. and M.M.R.-D.; Writing—Original Draft Preparation, D.L.-M. and M.M.R.-D.; Writing—Review and Editing, D.L.-M. and M.M.R.-D. All authors have read and agreed to the published version of the manuscript.

Institutional Review Board Statement: Not applicable.

Informed Consent Statement: Not applicable.

Data Availability Statement: The data presented in this study are available on request from the corresponding author.

Conflicts of Interest: Authors declare no conflict of interest, personal, financial, or otherwise, with the manuscript's material.

References

1. Colunga-GarcíaMarín, P.; Zizumbo-Villarreal, D.; Martínez-Torres, J. Tradiciones en el aprovechamiento de los agaves mexicanos: Una aportación a la protección legal y conservación de su diversidad biológica y cultural. In *En lo Ancestral Hay Futuro: Del Tequila, Los Mezcales y Otros Agaves*; Colunga-GarcíaMarín, P., Larqué-Saavedra, A., Eguiarte, L.E., Zizumbo-Villarreal, D., Eds.; Cicy-Conacyt-conabio-ine: Yucatán, México, 2007; pp. 229–248.
2. De León-Rodríguez, A.; González-Hernández, L.; Barba de la Rosa, A.P.; Escalante-Minakata, P.; López, G.M. Characterization of Volatile Compounds of Mezcal, and Ethnic Alcoholic Beverage Obtained from Agave salmiana. *J. Agric. Food Chem.* **2006**, *54*, 1337–1341. [CrossRef] [PubMed]
3. Lappe-Oliveras, P.; Moreno-Terrazas, R.; Arrizón-Gaviño, J.; Herrera-Suárez, T.; García-Mendoza, A.; Gschaedler-Mathis, A. Yeasts Associated with the Production of Mexican Alcoholic Nondistilled and Distilled Agave Beverages. *FEMS Yeast Res.* **2008**, *8*, 1037–1052. [CrossRef] [PubMed]
4. Vera-Guzmán, A.M.; Santiago-García, P.A.; López, M.G. Compuestos Volátiles Aromáticos Generados durante la Elaboración de Mezcal de Agave angustifolia y Agave potatorum. *Rev. Fitotec. Mex.* **2009**, *32*, 273–279. [CrossRef]
5. Vera-Guzmán, A.M.; López, M.G.; Hávez-Servia, J.L. Chemical Composition and Volatile Compounds in the Artisanal Fermentation of Mezcal in Oaxaca, Mexico. *Afr. J. Biotechnol.* **2012**, *11*, 14344–14353. [CrossRef]
6. Martell, N.M.A.; Córdova, G.E.E.; López, M.J.; Soto, C.N.O.; López, P.M.G.; Rutiaga, Q.O.M. Effect of Fementation Temperature on Chemical Composition of Mescals Made from Agave duranguensis Juice with Different Native Yeast Genera. *Afr. J. Microbiol. Res.* **2011**, *4*, 3669–3676.
7. Kirchmayr, M.R.; Segura-García, L.E.; Lappe-Oliveras, P.; Moreno-Terrazas, R.; De la Rosa, M.; Mathis, A.G. Impact of Environmental Conditions and Process Modifications on Microbial Diversity, Fermentation Efficiency and Chemical Profile during the Fermentation of Mezcal in Oaxaca. *LWT Food Sci. Technol.* **2017**, *79*, 160–169. [CrossRef]
8. Pisarnitskii, A. Formation of wine aroma: Tones and imperfections caused by minor components. *Appl. Biochem. Microbiol.* **2001**, *37*, 552–560. [CrossRef]
9. Cristiani, G.; Monnet, V. Food microorganisms and aromatic ester synthesis. *Sci. Aliment.* **2001**, *21*, 211–230. [CrossRef]
10. Swiegers, J.H.; Pretorius, I.S. Yeast modulation of wine flavor. *Adv. Appl. Microbiol.* **2005**, *57*, 131–175.
11. Genva, M.; Kenne Kemene, T.; Deleu, M.; Lins, L.; Fauconnier, M.L. Is It Possible to Predict the Odor of a Molecule on the Basis of Its Structure? *Int. J. Mol. Sci.* **2019**, *20*, 3018. [CrossRef]
12. Meilgaard, M. Flavor chemistry of beer: Part I: Flavor interaction between principal volatiles. *MBAA Tech. Q.* **1975**, *12*, 107–117.
13. Vera-Guzmán, A.M.; Guzmán-Gerónimo, R.I.; López, M.G.; Chávez-Servia, J.L. Volatile compound profiles in mezcal spirits as influenced by agave species and production processes. *Beverages* **2018**, *4*, 9. [CrossRef]
14. Ceballos-Magana, S.G.; Jurado, J.M.; Martin, M.J.; Pablos, F. Quantitation of twelve metals in tequila and Mezcal spirits as authenticity parameters. *J. Agric. Food Chem.* **2009**, *57*, 1372–1376. [CrossRef]
15. El Kazzy, M.; Weerakkody, J.S.; Hurot, C.; Mathey, R.; Buhot, A.; Scaramozzino, N.; Hou, Y. An overview of artificial olfaction systems with a focus on surface plasmon resonance for the analysis of volatile organic compounds. *Biosensors* **2021**, *11*, 244. [CrossRef]
16. Arshak, K.; Moore, E.; Lyons, G.M.; Harris, J.; Clifford, S.A. Review of Gas Sensors Employed in Electronic Nose Applications. *Sens. Rev.* **2004**, *24*, 181–198. [CrossRef]
17. Bauer-Christoph, C.; Christoph, N.; Aguilar-Cisneros, B.O.; López, M.G.; Richling, E.; Rossmann, A. Authentication of tequila by gas chromatography and stable isotope ratio analyses. *Eur. Food Res. Technol.* **2003**, *217*, 438–443. [CrossRef]
18. Peña-Alvarez, A.; Díaz, L.; Medina, A.; Labastida, C.; Capella, S.; Vera, L.E. Characterization of three agave species by gas chromatography and solid-phase microextraction-gas chromatography–mass spectrometry. *J. Chromatogr. A* **2004**, *1027*, 131–136. [CrossRef] [PubMed]
19. Lachenmeier, D.W.; Richling, E.; López, M.G.; Frank, W.; Scheier, P. Multivariate analysis of FTIR and ion chromatographic data for the quality control of tequila. *J. Agric. Food Chem.* **2005**, *53*, 2151–2157. [CrossRef]
20. Fraustro-Reyes, C.; Medina-Gutierrez, C.; Sato-Berru, R.; Sahagún, L.R. Qualitative study of etanol content in tequilas by Raman spectroscopy and principal component analysis. *Spectroschim. Acta Part A Mol. Biomol. Spectrosc.* **2005**, *61*, 2657–2662. [CrossRef]
21. Barbosa-García, O.; Ramos-Ortiz Maldonado, J.L.; Pichardo-Molina, J.L.; Meneses-Nava, M.A.; Landgrave, J.E.A. UV–vis absorption spectroscopy and multivariate analysis as a method to discriminate tequila. *Spectroschim. Acta Part A Mol. Biomol Spectrosc.* **2007**, *66*, 129–134. [CrossRef]
22. Brenet, S.; John-Herpin, A.; Gallat, F.-X.; Musnier, B.; Buhot, A.; Herrier, C.; Rousselle, T.; Livache, T.; Hou, Y. Highly-Selective Optoelectronic Nose Based on Surface Plasmon Resonance Imaging for Sensing Volatile Organic Compounds. *Anal. Chem.* **2018**, *90*, 9879–9887. [CrossRef] [PubMed]

23. Weerakkody, J.S.; Brenet, S.; Livache, T.; Herrier, C.; Hou, Y.; Buhot, A. Optical Index Prism Sensitivity of Surface Plasmon Resonance Imaging in Gas Phase: Experiment versus Theory. *J. Phys. Chem. C.* **2020**, *124*, 3756–3767. [CrossRef]

24. Gaggiotti, S.; Hurot, C.; Weerakkody, J.S.; Mathey, R.; Buhot, A.; Mascini, M.; Hou, Y.; Compagnone, D. Development of an Optoelectronic Nose Based on Surface Plasmon Resonance Imaging with Peptide and Hairpin DNA for Sensing Volatile Organic Compounds. *Sens. Actuators B Chem.* **2020**, *303*, 127188. [CrossRef]

25. Daly, S.M.; Grassi, M.; Shenoy, D.K.; Ugozzoli, F.; Dalcanale, E. Supramolecular Surface Plasmon Resonance (SPR) Sensors for Organophosphorus Vapor Detection. *J. Mater. Chem.* **2007**, *17*, 1809–1818. [CrossRef]

26. Liedberg, B.; Nylander, C.; Lundstrom, I. Biosensing with surface plasmon resonance—How it all started. *Biosens. Bioelectron.* **1995**, *10*, 1–9. [CrossRef]

27. Mezcal Gracias a Dios. Gracias a Dios Mezcal [Internet]. Available online: https://www.thankgad.com/ (accessed on 31 October 2022).

28. McPeak, K.M.; Jayanti, S.V.; Kress, S.J.; Meyer, S.; Iotti, S.; Rossinelli, A.; Norris, D.J. Plasmonic Films Can Easely Be Better: Rules and Recipes. *ACS Photonics* **2015**, *2*, 326–333. [CrossRef]

29. Macleod, H.A. *Thin Film Optical Filters*, 3rd ed.; Academic Press: Cambridge, MA, USA, 2001; Volume 4, 1967p.

30. Luna-Moreno, D.; Sánchez, Y.E.; de León, Y.P.; Arias, E.N.; Campos, G. Virtual instrumentation in LabVIEW for multiple optical characterizations on the same opto-mechanical system. *Optik (Stuttg)* **2015**, *126*, 1923–1929. [CrossRef]

31. Pronk, J.T.; Steensma, H.Y.; Van Dijken, J.P. Pyruvate metabolism in Saccharomyces cerevisiae. *Yeast* **1996**, *12*, 1607–1633. [CrossRef]

32. Liu, S.Q.; Quek, A.Y.H. Evaluation of Beer Fermentation with a Novel Yeast Williopsis saturnus. *Food Technol. Biotechnol.* **2016**, *54*, 403. [CrossRef]

33. Arrizon, J.; Gschaedler, A. Increasing fermentation efficiency at high sugar concentrations by supplementing an additional source of nitrogen during the exponential phase of the tequila fermentation process. *Can. J. Microbiol.* **2002**, *48*, 965–970. [CrossRef]

34. Arrizon, J.; Gschaedler, A. Effects of the addition of different nitrogen sources in the tequila fermentation process at high sugar concentration. *J. Appl. Microbiol.* **2007**, *102*, 1123–1131. [CrossRef] [PubMed]

35. Berry, D.R.; Watson, D.C. Production of organoleptic compounds. In *Yeast Biotechnology*; Berry, D.R., Russell, I., Stewart, G.G., Eds.; Springer: Dordrecht, The Netherlands, 1987; pp. 345–368.

36. Martínez-Aguilar, J.F.; Peña-Álvarez, A.J. Characterization of Five Typical Agave Plants used to Produce Mezcal through their Simple Lipid Composition Analysis by Gas Chromatography. *J. Agric. Food Chem.* **2009**, *57*, 1933–1939. [CrossRef] [PubMed]

37. Ding-Wei, H. Approach the angular sensitivity limit in surface plasmon resonance sensors with low index prism and large resonant angle. *Opt. Eng.* **2010**, *49*, 054403.

38. Weast, R.C. *Handbook of Chemistry and Physics*, 49th ed.; Weast, R.C., Ed.; Chemical Rubber Publishing Company: Cleveland, OH, USA, 1969; p. 423.

39. Lynch, D.W.; Huttner, W.R. *Handbook of Optical Constants of Solids*; Palik, E.D., Ed.; Academic Press: New York, NY, USA, 1980; pp. 275–367.

40. Ekgasit, S.; Tangcharoenbumrungsuk, A.; Yu, F.; Baba, A.; Knoll, W. Resonance shifts in SPR curves of nonabsorbing, weakly absorbing, and strongly absorbing dielectrics. *Sens. Actuators B Chem.* **2005**, *105*, 532–541. [CrossRef]

41. Ortega, J. Densities and refractive indices of pure alcohols as a function of temperature. *J. Chem. Eng. Data* **1982**, *27*, 312–317. [CrossRef]

42. Luna-Moreno, D.; Monzón-Hernández, D.; Noé-Arias, E.; Regalado, L.E. Determination of quality and adulteration of tequila through the use of surface plasmon resonance. *Appl. Opt.* **2012**, *51*, 5161–5167. [CrossRef]

43. Leite, I.; Navarrete, M.C.; Díaz-Herrera, N.; González-Cano, A.; Esteban, Ó. Selectivity of SPR fiber sensors in absorptive media: An experimental evaluation. *Sens. Actuators B Chem.* **2011**, *160*, 592–597. [CrossRef]

44. Panda, A.; Pukhrambam, P.D.; Keiser, G. Performance analysis of graphene-based surface plasmon resonance biosensor for blood glucose and gas detection. *Appl. Phys. A* **2020**, *126*, 1–12. [CrossRef]

45. Gupta, B.D.; Verma, R.K. Surface plasmon resonance-based fiber optic sensors: Principle, probe designs, and some applications. *J. Sens.* **2009**, *2009*, 979761. [CrossRef]

46. Maharana, P.K.; Srivastava, T.; Jha, R. On the performance of highly sensitive and accurate graphene-on-aluminum and silicon-based SPR biosensor for visible and near infrared. *Plasmonics* **2014**, *9*, 1113–1120. [CrossRef]

47. Sharma, A.K.; Jha, R.; Gupta, B.D. Fiber-optic sensors based on surface plasmon resonance: A comprehensive review. *IEEE Sens. J.* **2007**, *7*, 1118–1129. [CrossRef]

48. Mishra, A.K.; Mishra, S.K.; Verma, R.K. An SPR-based sensor with an extremely large dynamic range of refractive index measurements in the visible region. *J. Phys. D Appl. Phys.* **2015**, *48*, 435502. [CrossRef]

49. Fu, H.; Zhang, S.; Chen, H.; Weng, J. Graphene enhances the sensitivity of fiber-optic surface plasmon resonance biosensor. *IEEE Sens. J.* **2015**, *15*, 5478–5482. [CrossRef]

50. Dillon, M.; Zaczek-Moczydlowska, M.A.; Edwards, C.; Turner, A.D.; Miller, P.I.; Moore, H.; McKinney, A.; Lawton, L.; Campbell, K. Current trends and challenges for rapid smart diagnostics at point-of-site testing for marine toxins. *Sensors* **2021**, *21*, 2499. [CrossRef] [PubMed]

51. Hill, R.T. Plasmonic biosensors. *Interdiscip. Rev. Nanomed. Nanobiotechnol.* **2015**, *7*, 152–168. [CrossRef] [PubMed]

52. Koyun, A.; Ahlatcolu, E.; Koca, Y.; Kara, S. Biosensors and their principles. In *A Roadmap of Biomedical Engineers and Milestones*, 1st ed.; Kara, S., Ed.; InTech-Janeza Trdine: Rijeka, Croatia, 2012; pp. 117–142.

53. Zuppolini, S.; Quero, G.; Consales, M.; Diodato, L.; Vaiano, P.; Venturelli, A.; Santucci, M.; Spyrakis, F.; Costi, M.P.; Giordano, M.; et al. Label-free fiber optic optrode for the detection of class C β-lactamases expressed by drug resistant bacteria. *Biomed. Opt. Express* **2017**, *8*, 5191–5205. [CrossRef]

54. Grieshaber, D.; MacKenzie, R.; Vörös, J.; Reimhult, E. Electrochemical biosensors-sensor principles and architectures. *Sensors* **2008**, *8*, 1400–1458. [CrossRef]